Available online at www.derpharmachemica.com

Scholars Research Library

Der Pharma Chemica, 2015, 7(9):307-321
(http://derpharmachemica.com/archive.html)

ISSN 0975-413X
CODEN (USA): PCHHAX

Docking, dynamic simulation and quantum mechanics studies of pyrazinamide derivatives as novel inhibitors of Acetylcholinesterase and Butyrylcholinesterase

Ismail Daoud[1,2*], Smail Bouarab[1,3] and Said Ghalem[2]

[1]*University Mohamed khider- Biskra- Algeria*
[2]*Laboratory of Natural Substances and Bioactive (LASNABIO), University Abou-Bakr Belkaid-Faculty of Science-Department of Chemistry- Tlemcen- Algeria*
[3]*Laboratory of Theoretical Chemistry Computational and Photonic (LCTCP).University USTHB, Department of Chemistry –Algeria*

ABSTRACT

Several cholinesterase (Acetylcholinesterase and Butyrylcholinesterase) inhibitors are either being utilized for symptomatic treatment of Alzheimer's disease or are in advanced clinical trials. A series of 12 known pyrazinamide derivatives that display inhibitory activity toward both acetylcholinesterase and butyrylcholinesterase (ChEs) was considered for theoretical studies. These theoretical approaches employed quantum mechanics and molecular docking data from both ChEs that were previously submitted to molecular dynamics (MD) simulations. Docking studies revealed that the complex formed between ChEs and the best pyrazinamide derivatives compounds reproduced the binding mode for theoretical calculation reported, where the ligand was coupled into the choline-binding site and stabilized through the hydrogen bonds interactions with Tyr121 or Tyr332 for AChE and BuChE, respectively, suggesting that these compounds could be an efficients inhibitors. The careful analysis of the investigation gave the compounds L_3 and L_4 as the most promising compounds based on the docking score energies and hydrogen bonds distances. The best possible interactions of the lead compounds are simulated for stability using molecular dynamics. The results of this investigation provide valuable information on the design of highly selective pyrazinamide derivatives.

Keywords: Butyrylcholinesterase, Acetylcholinesterase, pyrazinamide, Inhibitors, DFT, Docking study.

INTRODUCTION

Alzheimer's disease (AD) is a neurodegenerative disorder that based on the World Health Organization (WHO) report, has affected more than 37 million people worldwide [1]. As a progressive neurodegenerative disease, AD is characterized by multiple cognitive impairments including gradual loss of memory, judgment and learning ability owing to loss of neurons and synapses in the certain sub-cortical regions and cerebral cortex [2,3]. It is not yet clear which structures are essential for the pathogenesis of AD. There are two characteristic features which are present in the brains of AD patients: neurofibrillar tangles and Amyloid β(Aβ) plaques [4].

Recently, the genesis of amyloid protein plaques has been associated with some alterations of both Acetylcholinesterase (AChE, E.C. 3.1.1.7) and Butyrylcholinesterase (BuChE, E.C. 3.1.1.8), given that by using ChE inhibitors such plaques decrease considerably in patients with AD [5-7].

Both cholinesterase enzymes acetylcholinesterase (AChE) and butyrylcholinesterase (BuChE) are involved in the hydrolysis of acetylcholine; however, studies showed that as the disease progresses, the activity of AChE decreases

while the activity of BuChE remains unaffected or even increases [8]. In the normal brain, AChE predominates over BuChE activity [9]. However, some evidences suggest that inhibition of brain BuChE may represent an important therapeutic target for AD. It is reported that the BuChE has a key role that can partly compensate for the action of AChE [10]. Cholinesterase inhibitors have been approved as efficacious treatment to reduce the symptoms of early medium stage of AD. Several antiacetylcholinesterase agents such as donepezil [11], tacrine [12], galantamine [13], and ensaculin [14] have shown to induce modest improvement inmemory and cognitive functions. The development of specific small molecule drugs BuChE inhibitors with the capability to inhibit BuChE together with AChE should lead to better clinical outcomes [15].

The chemical structure of pyrazinamide provides a most valuable molecular template for the development of agents able to interact with a wide variety of biological activities [16].

Pyrimidine derivatives comprise a diverse and interesting group of drugs is extremely important for their biological activities. Dihydropyrimidine and their derivatives have attracted increasing interest owing to their therapeutic and pharmaceutical properties, such as antiviral, antitubercular [17,18], antimicrobial agent [19–23] antagonists of the human adenosine A2A receptor [24], cyclooxygenase-2 inhibitory activity [25,26], tyrosine kinase inhibitors, antiamoebic activity [27,28], cytotoxicity [29,30] and acetyl cholinesterase inhibitor activity [31].

Recently, a series of novel pyrazinamide condensed 1,2,3,4-tetrahydropyrimidines were synthesized and evaluated showed the best AChE and BuChE inhibitory activity [32].

In the light of these findings, molecular modeling plays an important role in the rational drug design and is used to predict the bonding affinity, spatial orientation and total binding energy the structure of pyrazinamide molecule drug candidates to the active site of their target enzymes. All final compounds were tested and evaluated against cholinesterases (AChE and BuChE). In order to predict the binding modes of the new active inhibitors molecular docking studies were carried out by using Molegro Virtual Docker (MVD2012) docking software's. While to check the stability of the ligands inside the enzymes, molecular dynamic simulations (MDs) was conducted by using HyperChem07 software.

2. Preparation of ligands and enzymes

2.1. Ligands structures

First, the 1,2,3,4-tetrahydropyrimidines (see Table 1) structures were optimized by using MM+ molecular modeling and the semi-empirical AM1 method, both of which are implemented in Hyperchem 7.0 software [33]. For these calculations, the Polak-Ribiere conjugate gradient algorithm was employed, with the RMS gradient set to 0.0001 kcal/Å mol. The chemical properties of ligands are given in see Table 2

Table 1 : Synthesized 1,2,3,4-tetrahydropyrimidines : in vitro acetyl and butyl cholinesterase inhibitor activity [32]

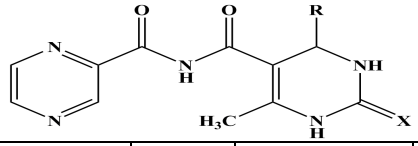

Ligands	R	X	AChE IC50(µM)±SEM	BuChE IC50(µM)±SEM
L_1	Phenyl	O	5.35±0.01	7.21±0.01
L_2	Phenyl	S	5.26±0.01	6.75±0.01
L_3	3-Nitorophenyl	O	2.54±0.01	5.93±0.01
L_4	3-Nitorophenyl	S	1.82±0.01	5.38±0.01
L_5	3-chlorophenyl	O	1.21±0.01	4.96±0.01
L_6	3-chlorophenyl	S	1.05±0.01	4.31±0.01
L_7	4-Flurophenyl	O	0.86±0.01	4.84±0.01
L_8	4-Flurophenyl	S	0.75±0.01	3.93±0.01
L_9	4-Chlorophenyl	O	0.94±0.01	4.75±0.01
L_{10}	4-Chlorophenyl	S	0.88±0.01	4.13±0.01
L_{11}	4-Pyridyl	O	0.19±0.01	3.92±0.01
L_{12}	4-Pyridyl	S	0.11±0.01	3.46±0.01
L_{13}	Donepezil HCl	Standard	0.13±0.01	3.58±0.01
$L_{13'}$	BCH_604	Standard	-	-

Table 2 : Chemical properties of ligands

Ligands	Number of atoms	Number of heavy atoms	Number of bonds	Molecular weight	Flexible torsions
L_1	40	25	42	337.333	3 (out of 3)
L_2	40	25	42	353.398	3 (out of 3)
L_3	42	28	44	382.330	4 (out of 4)
L_4	42	28	44	398.396	4 (out of 4)
L_5	40	26	42	371.778	3 (out of 3)
L_6	40	26	42	387.843	3 (out of 3)
L_7	40	26	42	355.323	3 (out of 3)
L_8	40	26	42	371.389	3 (out of 3)
L_9	40	26	42	371.778	3 (out of 3)
L_{10}	40	26	42	387.843	3 (out of 3)
L_{11}	39	25	41	338.321	3 (out of 3)
L_{12}	39	25	41	354.386	3 (out of 3)
L_{13}	57	28	60	379.492	6 (out of 6)
$L_{13'}$	31	12	30	189.318	5 (out of 5)

2.2. Enzymes structures

The X-ray crystal structures of both cholinesterase AChE (PDB ID: 1EVE) [34], and BuChE (PDB ID: 1P0P) [35] were downloaded from RCSB Database (www.rcsb.org/pdb) [36].

1EVE is a three dimensional structure of the anti-alzheimer drug, e2020 (aricept), complexed with its target Acetylcholinesterase with EC Number: 3.1.1.7 classified Serine Hydrolase under class of enzymes, complexed with a selective inhibitor E20 with 1 chains (A), 2.50 Å resolution and 0.188 R-value respectively. 1P0P is a three dimensional structure of the anti-alzheimer drug with EC Number: 3.1.1.8 classified Hydrolase under class of enzymes of Butyrylcholinesterase complexed with a selective inhibitor BCH_604($C_9H_{20}NOS$) with 1 chain, 2.30 Å resolution and 0.199 R-value respectively. Table 3 shows other propriety of both enzymes.

Table 3 : propriety of enzymes pdb: 1EVE and 1P0P

	Number of residues	Number of atoms	Number of heavy atoms	Number of bonds	Molecular weight
1EVE	**534**	8361	4254	8487	60238.6
1P0P	**522**	8235	4157	8354	58746.3

Computational analysis was carried out on chain A of both enzymes 1EVE and 1P0P. The twelve molecules $\mathbf{L_{1\text{-}12}}$ were selected to study the associated physico-chemical parameters and protein-ligands interactions.

To obtain better potential binding sites in the 1EVE and 1P0P, a maximum of five cavities was detected using default parameters. The volume and surface of cavities are showed in Table 4.

Table 4 : Volume and surface of five cavities detected by MolDock Score

	1EVE		1P0P	
Cavities	**Volumes (Å^3)**	**Surfaces (Å^2)**	**Volumes (Å^3)**	**Surfaces (Å^2)**
1	**235.008**	**613.12**	**392.704**	**1254.4**
2	119.296	441.60	354.816	688.64
3	68.608	257.28	114.688	435.20
4	43.520	171.52	49.664	216.32
5	30.208	117.76	44.032	144.64

It found that the ligand co-crystallize selective inhibitor (L_{13}:C_{24} H_{29} N O_3) of 1EVE is fixed in cavity 1 (V=235.008Å^3, S=613.12Å^2). Out of the detected cavities, cavity 1 was selected for further studies in two cases for our study (see Figure 1).

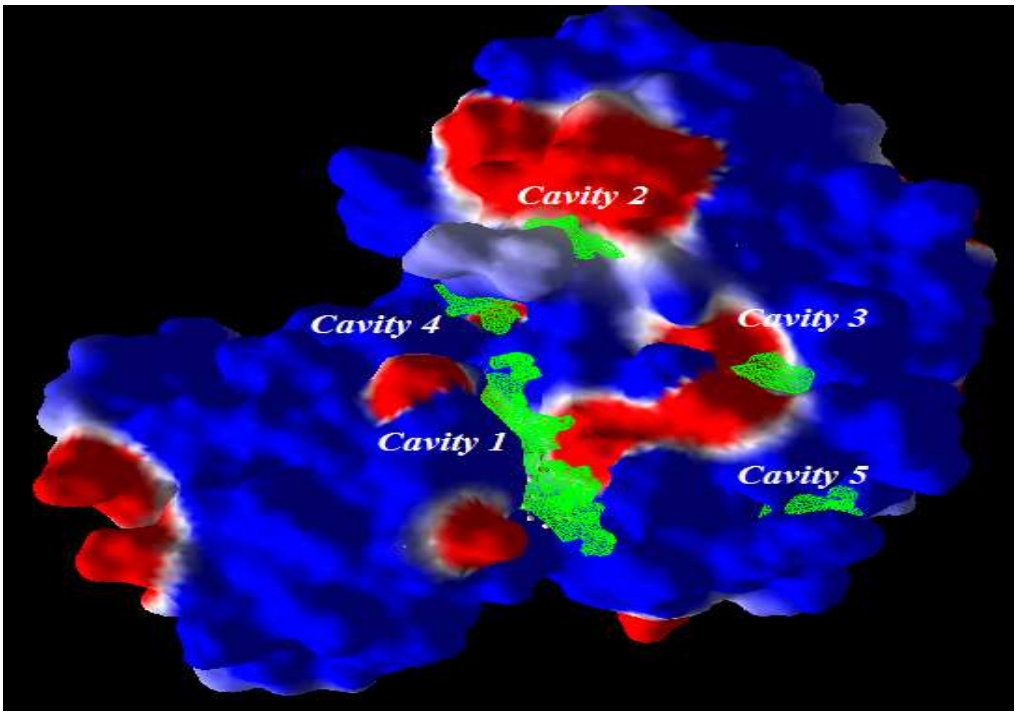

Figure 1: cavities detected by MolDock Score for 1EVE (green color)

3. Computational procedure

3.1. Molecular dynamics

Classical MD simulations of ligands and both enzymes were performed using the HyperChem 07 program employing the MM+ force field in the case of ligands [33] and Amber in the case of enzymes [37].

For calculation of molecular dynamics details, the equilibration protocol consisted of 1500 minimization steps, followed by 30 ps of MD simulations at 10 K with fixed protein atoms. Subsequently, the entire system was minimized over 1500 steps (at 0 K), followed by gradual heating from 10 to 310 K using temperature reassignment during the initial 10 ps of the 500 ps equilibration dynamics without restraints.

3.2. Docking simulations

The initial ChEs coordinates were obtained from the PDB (PDB IDs: **1EVE** and **1P0P**). The co-crystallized ligands and water molecules of the crystal structure were removed, and the hydrogen atoms were added using the Chimera 1.8 software [38].

For docking studies, we utilized several protein conformations previously obtained through the MD simulation procedures mentioned above.

The structure of the protein was corrected for missing atoms or unknown units using Molegro Virtual Docker (MVD2012) program [39], graphical-automatic software (http://molegro.com/mvd-product.php). All solvent molecules and the co-crystallized inhibitor were removed from the structures to provide sterically unimpeded cavities for ligand docking.

Docking was performed by using Molegro Virtual Docker (MVD) software package because this algorithm maintains a rigid macromolecule while allowing ligand flexibility. This program has been widely used because it displays good free energy correlation values between docking simulations and experimental data in more, it have been a high accuracy than other programs [40].

The identification of ligand binding modes is done by iteratively evaluating a number of candidate solutions (ligand conformations) and estimating the energy of their interactions with the macromolecule. MVD performs flexible ligand docking, so the optimal geometry of the ligand will be determined during the docking. The MolDock scoring function (MolDock Score) used by MVD is derived from the PLP scoring functions originally proposed by Gehlhaar et al and later extended by Yang et al [41]. The MolDock scoring function further improves these scoring functions with a new hydrogen bonding term and new charge schemes.

3.3. Quantum studies

First, the 1,2,3,4-tetrahydropyrimidines (Table 1) structures were optimized by using MM+ molecular modeling and the semi-empirical AM1 method, both of which are implemented in Hyperchem 7.0 soft- ware [33]. Afterwards, as well as density functional theory (DFT) [42] calculations implemented in the Gaussian 09 program were performed [43,44]. Thus, the structures obtained were fully optimized at the DFT/B3LYP/6-31G(d) level of theory [45–49], followed by single-point calculations at the same level of theory [50–51]. Calculated vibrational frequencies ensured that the structures were stable (with no imaginary frequencies).

On the other hand, the electronic properties for our ligands have been calculated, including electronic chemical potential [52], (1) Ionization Potential (IP), (2) Gap (HOMO-LUMO), (3) Dipole Moment (M) and (4) Energy (HF) [53,54], as well as the energy of the highest occupied molecular orbital (HOMO) and the lowest unoccupied molecular orbital (LUMO).

RESULTS AND DISCUSSION

Theoretical studies (dynamic simulation, docking and quantum chemistry) were performed for 12 ligands (1,2,3,4-tetrahydropyrimidine derivatives) and re-dock for ligand co-cristalized (L_{13} and $L_{13'}$), considering that several compounds with related structures have activities as AChE inhibitors (see Table1). The docking studies suggest that all the tested compounds bind at the active site of both ChEs. This could be due to the fact that they have an aromatic ring and a nitrogen atom, like other ChE inhibitors [32]. In the other hand, perhaps there are several functional groups that modify the electronic density on the aromatic ring and the N atom, which might change the affinity between the ligands and the enzymes. Docking calculations allow predicting the structure of all the complexes between the enzymes and the ligands, thus suggesting the kind of interaction (Van der Walls, steric and hydrogen…) and the energy obtained by calculation.

4.1. Molecular dynamics

The MD protocol involved a three-step minimization, followed by a pre-production step, and finally production MD simulations.

MD simulations used to study two protein flexibility properties, the variation of the potential energy of both enzymes according to time given in the figure 2. In this figure the geometrical parameters calculated through the 90 ps-long MD simulations of both ChEs.

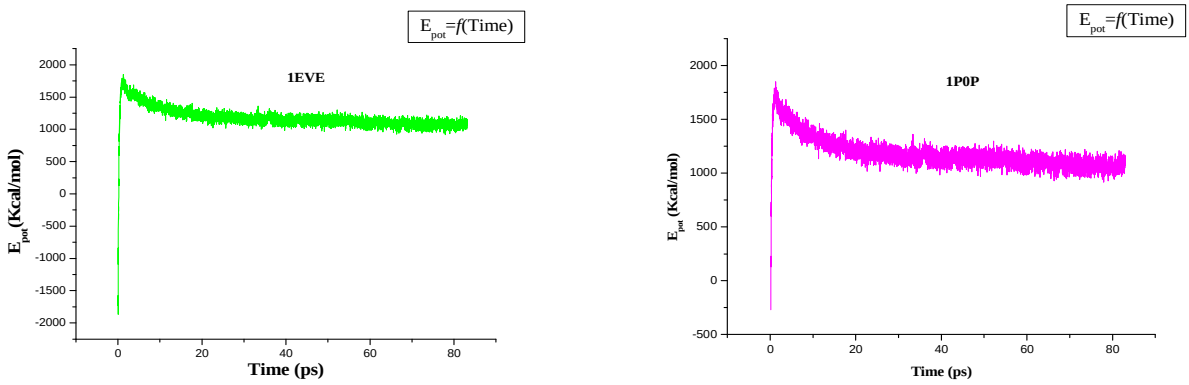

Figure 2 : Variation of the potential energy of the both enzymes according to time

MD simulations serve to study ligands flexibility properties; the figure 3 shows the variation of the potential energy of the ligands according to time, in this case geometrical parameters calculated through the 500 ps-long MD simulations of ligands.

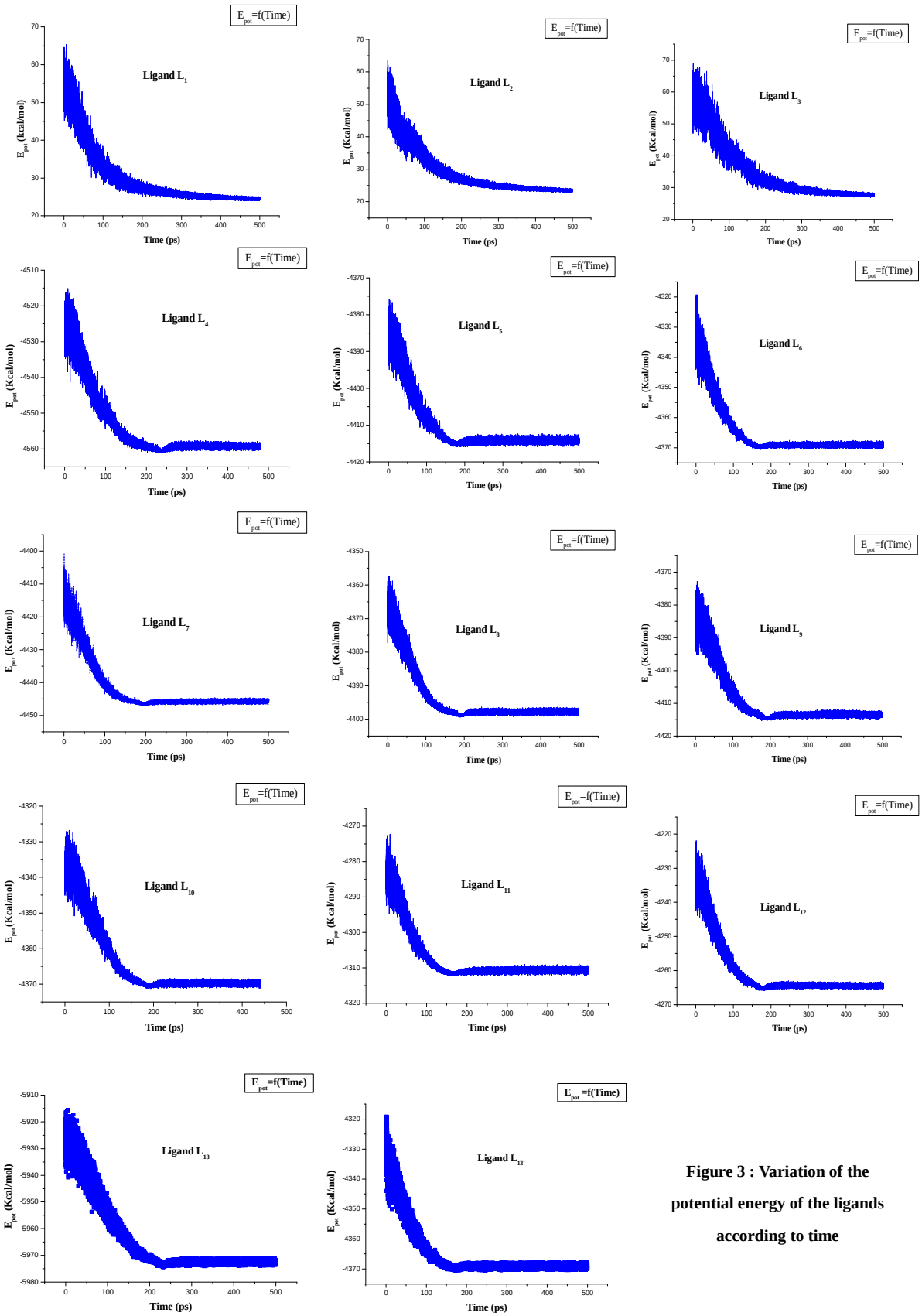

Figure 3 : Variation of the potential energy of the ligands according to time

The MD simulations of the both enzymes (1EVE and 1P0P) orients in a different conformation. These results give a conformation favorable and also the most flexible parts for the two enzymes. In the other hand, molecular dynamics helps us to find the maximum interactions between the ligands and enzymes. It is observed that the two graphs of the both enzymes (see Figure 2) shows a stability of potential energy of the ligands according to time, this may be indicate that DM help us to obtain the local minima.

According to graphs' obtained in figure 3, we notice that energy potential of the ligands stabilizes according to time this proves that we can obtained the most stable conformation.

4.2. Quantum studies

First, the energy of each series of compounds was obtained from the single-point calculations performed at the DFT/B3LYP/6-31G(d) theory level with the B3LYP/6-31G(d) geometries. Using a higher basis set in the single point calculations, we obtained a better energy value that those reported in the Table 5.

Table 5 : HOMO and LUMO energies (u.a), HOMO-LUMO gaps (u.a), Dipole Moment M (Debye), Ionization Potential IP (u.a), energy (HF) (u.a) for compounds

LIGANDS	HOMO	LUMO	Gap	M	IP	Energies
L_1	-0.2338	-0.0730	-0.1608	5.1774	0.2338	-1156.2900
L_2	-0.2118	-0.0848	-0.1270	6.2276	0.2118	-1479.2484
L_3	-0.2220	-0.0940	**-0.1280**	2.2217	0.2220	-1469.2451
L_4	-0.2306	-0.1016	**-0.1290**	2.4008	0.2306	-1683.7526
L_5	-0.2355	-0.0840	-0.1515	4.8492	0.2355	-1615.8982
L_6	-0.2225	-0.0891	-0.1334	2.5783	0.2225	-1938.8426
L_7	-0.2227	-0.0891	-0.1336	2.6951	0.2227	-1928.8345
L_8	-0.2244	-0.0859	-0.1385	2.6614	0.2244	-1578.4856
L_9	-0.2287	-0.0895	-0.1392	4.0027	0.2287	-1615.9009
L_{10}	-0.2262	-0.0872	-0.1390	2.6028	0.2262	-1938.8484
L_{11}	-0.2383	-0.0846	-0.1537	2.9681	0.2383	-1172.3384
L_{12}	-0.2287	-0.0825	-0.1462	2.5715	0.2287	-1495.2870
L_{13}	-0.2015	-0.0474	-0.1541	2.9094	0.2015	-1212.4213 1212.4213
$L_{13'}$	-0.2019	-0.0555	-0.1464	2.7160	0.2019	-1222.5421

Also, we have calculated the HOMO, LUMO, Gap, Dipole Moment, Ionization Potential and energy (HF) of the Pyrimidine derivatives using the frontier molecular orbital information.

1u.a = 627.52 Kcal/mol = 27.21 eV.

The most important orbitals in a molecules are the frontier molecular orbitals, called highest occupied molecular orbital (HOMO) and lowest unoccupied molecular orbital (LUMO). These orbitals determine the way the molecule interacts with other species. The frontier orbital gap helps us to characterize the chemical reactivity and kinetic stability of the molecule. A molecule with a small frontier orbital gap is more polarizable and is generally associated with a high chemical reactivity, low kinetic stability and is also termed as soft molecule [55]. The HOMO is the orbital that primarily acts as an electron donor and the LUMO is the orbital that largely acts as the electron acceptor [56].

The analysis of the HOMO-LUMO energy gap values given in Table 5 show that all values are found between -0.1608 and -0.1260 u.a . In this case we noted that the lower value for frontier orbital gap (HOMO-LUMO) found in L_3 and L_4 than other ligands makes it slightly more reactive and less stable (Table 5).

Also the calculated results show that the Dipole Moment of L_3 and L_4 are much lower than the other ligands (see Table 5). On the other hand, we found that the lowest energy in ligands L_{10} (more stable than other ligands).

4.3. Molecular docking

In recent years, the pathogenesis of AD has been associated with both ChEs, resulting in several studies that have targeted these two enzymes [57-64]. The fact that both ChEs have some different structural characteristics and the anionic site and the catalytic triads are conserved at the gorge led us to hypothesize that Pyrimidine derivatives could act in the recognition site of both ChEs. Thus, drug design efforts were made with the initial idea that they would act on both ChEs with similar affinity.

The binding site cavity detection and docking simulation was performed by using docking software, namely MVD (Molegro Virtual Docker) for the selected Pyrimidine derivatives at Human cholinesterase AChE (PDB ID: 1EVE), and BuChE (PDB ID: 1P0P).

Flexible docking of ligands selected in this study was carried out in the active site of ChEs. Five top poses for each ligand were returned in the simulation, out of which one best pose for each ligand was selected on the basis of their MolDock score.

The results obtained using MVD, shown in terms of MolDockScore; Rerank Score, Interaction, H-bonding energy ; E-Intra (Steric), E-Intra (V.d.W) respectively are given in Table 6 and 7 (All values measured by kcal/mol).

Table 6 : Comparative docking simulation result of selected Pyrimidine derivatives (L_1-L_{13}) with Human cholinesterase AChE (PDB ID: 1EVE)

Ligands	Moldock Score[a]	Rerank Score	Interaction[b]	H-bond	E-Intra (Steric)	E-Intra (V.d.W)
L_1	-133.828	-59.870	-148.545	-7.056	14.194	65.424
L_2	-138.523	-108.660	-146.539	-5	6.275	69.634
L_3	**-179.586**	-135.44	-168.827	-7.690	-12.197	62.695
L_4	**-167.004**	-132.977	-173.053	-7.308	5.832	82.119
L_5	-143.770	-121.213	-158.630	-2.5	14.211	83.339
L_6	-163.488	-108.827	-151.750	-3.239	-13.613	69.826
L_7	-151.049	-123.805	-165.295	-4.283	13.766	80.265
L_8	-146.076	-116.606	-152.299	-2.656	5.426	77.788
L_9	-128.582	-103.116	-148.844	-3.118	19.505	100.812
L_{10}	-153.940	-117.613	-159.800	-7.063	3.879	67.060
L_{11}	-147.871	-94.407	-158.908	-15.445	10.582	66.558
L_{12}	-138.381	-117.829	-155.045	-4.117	16.482	79.777
L_{13}	**-154.773**	-126.692	-173.882	**-2.5**	10.799	75.48

[a]MolDock score calculated by summing the external ligand interaction (protein–ligand interaction) and internal ligand interaction score using Virtual Molecular Viewer 1.2.0.

[b] The total interaction energy between the pose and the target molecules(s).

Table 7 : Comparative docking simulation result of selected Pyrimidine derivatives (L_1-$L_{13'}$) with Human cholinesterase BuChE (PDB ID: 1P0P)

Ligands	Moldock Score	Rerank Score	Interaction	H-bond	E-Intra (Steric)	E-Intra (V.d.W)
L_1	-134.211	-114.272	-146.111	-10.644	11.196	65.954
L_2	-121.277	-93.822	-125.390	-3.813	3.135	65.746
L_3	**-155.428**	-108.055	-144.741	-5.037	-11.665	63.948
L_4	**-147.266**	-112.002	-152.990	-15.620	4.305	72.302
L_5	-132.439	-110.834	-147.196	-2.724	14.144	84.431
L_6	-140.148	-99.014	-127.473	-4.324	-13.450	70.336
L_7	-136.860	-118.549	-155.897	-3.577	18.838	82.459
L_8	**-141.748**	-117.824	-153.278	**-6.179**	10.022	74.196
L_9	-128.227	-101.79	-145.512	-6.979	16.876	91.737
L_{10}	-146.088	-115.327	-149.976	-3.121	2.877	65.139
L_{11}	-133.891	-110.998	-143.022	-7.298	8.908	67.412
L_{12}	-128.355	-106.847	-135.897	-2.5	7.253	72.266
$L_{13'}$	**-142.511**	-96.372	-152.59	**-2.50**	3.469	115.011

The high value the Flexible torsions (4 (out of 4), (see Table 2) of L_3 and L_4 ensures that they are able to undergo additional polar and nonpolar contacts within AChE and BuChE binding site compared to Donepezil (L_{13}) and BCH_604 ($L_{13'}$). Furthermore, the ligand-enzyme complex energy was calculated (Table 6 and Table 7) which suggests that L_3 and L_4 has the lowest binding energy (-179.586, -167.004 kcal/mol) with AChE and -155.428, -147.266 kcal/mol, with BuChE toward enzymes compared to Donepezil and BCH_604 (-154.773 and -142.511 kcal/ mol) respectively. Tables 6 and 7, shows active site residues and proves that a number of hydrogen bonds are involved in interaction between selected ligands (**L_1-$_{13}$**) with the receptor Human ChEs.

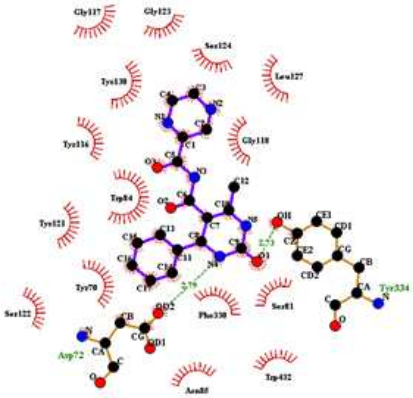

L1

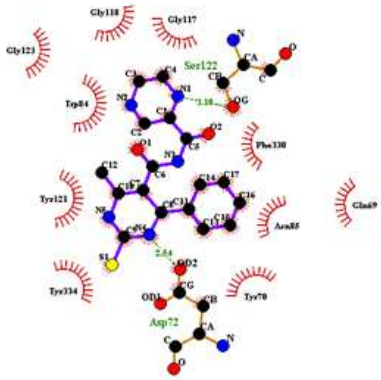

L2

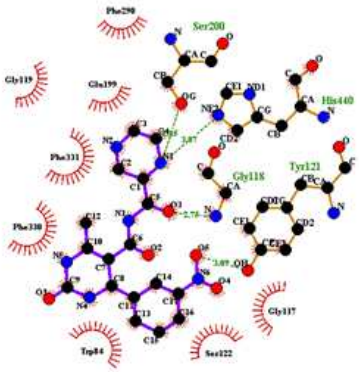

L3

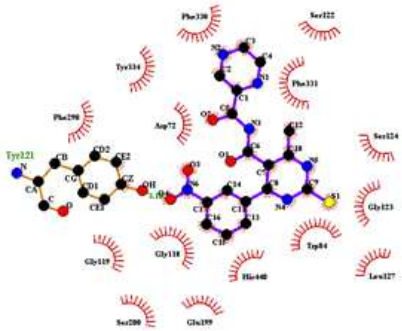

L4

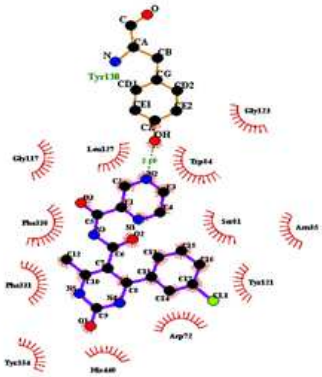

L5

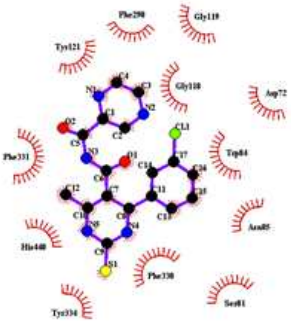

L6

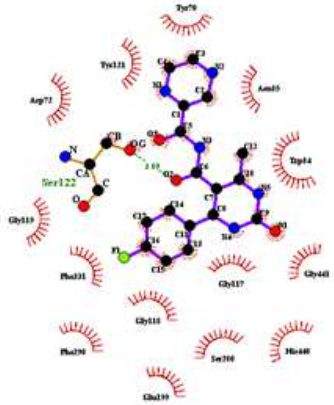

L7

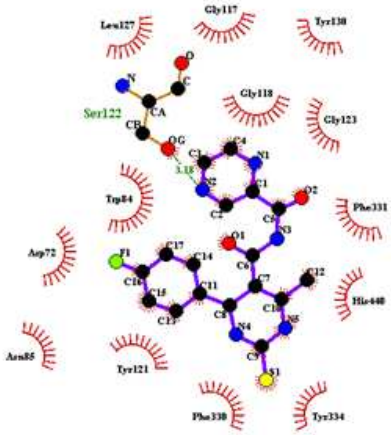

L8

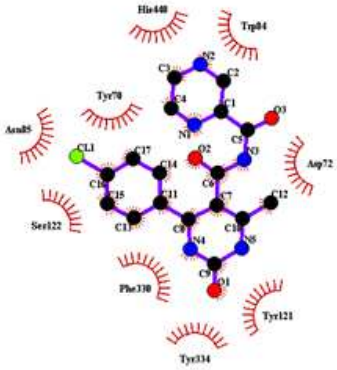

L9

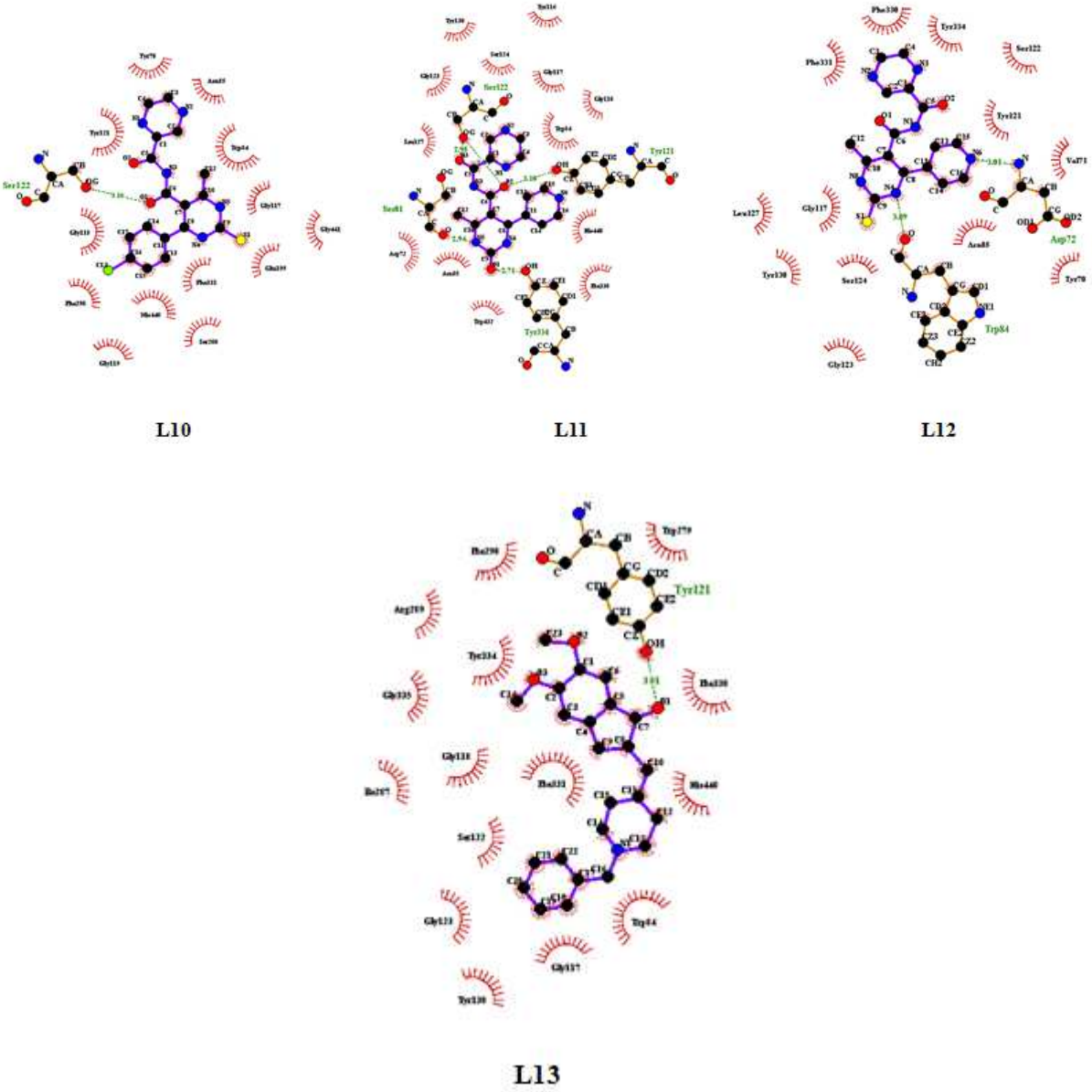

Figure 4 : Hydrogen bonds between ligands and residues of active site of 1EVE used LigPlot+ program [65].

Table 8 and Figure 4 show the hydrogen bonds (*Atom of compound, involved receptor atoms, involved receptor residues, Type of Hydrogen bond and distances*) between the docked ligand and the amino acids of AChE

Table 8 : Hydrogen bonds between atoms of compounds and amino acids of 1EVE

Compounds	*Atom of compound*	*Involved receptor atoms*	*Involved receptor residues*	*Type of Hydrogen bond*	*Distance (Å)*
L_1	O1	OH	Tyr334	H-don	2.73
	N4	OD	Asp72	H-don	2.79
L_2	N1	OG	Ser122	H-don	3.10
	N4	OD	Asp72	H-don	2.54
L_3	N1	OG	Ser200	H-don	2.85
	N1	NE	His440	H-acc	3.07
	O3	NE	Gly118	H-acc	2.75
	O5	OH	Tyr121	H-don	3.09
L_4	O4	OH	Tyr121	H-don	3.10
L_5	N2	OH	Tyr130	H-don	2.06
L_6	-	-	-	-	-
L_7	O2	OG	Ser122	H-don	3.09
L_8	N2	OG	Ser122	H-don	2.60
L_9	-	-	-	-	-
L_{10}	O1	OG	Ser122	H-don	3.10
L_{11}	O3	OG	Ser122	H-don	2.95
	O2	OG	Ser122	H-acc	3.84

	O2	OH	Tyr121	H-don	3.10
	N5	OH	Ser81	H-don	2.94
	O1	OH	Tyr334	H-don	2.71
L_{12}	N6	NE	Asp72	H-acc	3.01
	N4	OH	Trp84	H-don	3.09
L_{13}	O1	OH	Tyr121	H-don	3.01

Table 9 : Hydrogen bonds between atoms of compounds and amino acids of 1P0P

Compounds	*Atom of compound*	*Involved receptor atoms*	*Involved receptor residues*	*Type of Hydrogen bond*	*Distance (Å)*
L_1	N2	OG	Ser198	H-don	2.58
	O1	NE1	Trp82	H-acc	3.03
	O1	OH	Tyr440	H-don	2.97
	N5	OH	His438	H-don	3.09
L_2	N1	OG	Ser198	H-don	3.21
	N5	OH	His438	H-don	3.13
L_3	N2	OH	Tyr332	H-don	2.93
	N3	OH	His438	H-don	2.92
L_4	O2	OH	Tyr332	H-don	2.63
	O3	OG	Ser198	H-acc	2.64
	O3	N	Gly117	H-don	2.83
	O3	N	Gly116	H-don	2.60
	N5	OG1	Thr120	H-don	2.94
L_5	N2	OG1	Thr120	H-don	2.78
L_6	O1	OG1	Thr120	H-don	2.95
	N4	NE2	His438	H-don	3.15
L_7	O1	OG1	Asp70	H-don	3.04
	N4	NE2	Thr120	H-don	2.78
L_8	N1	N	Asp70	H-don	2.97
	N5	OH	Tyr128	H-don	2.92
	S1	OH	Tyr128	H-don	2.89
	O1	OG1	Thr120	H-don	2.48
L_9	N5	OH	His438	H-don	2.89
	O2	NE2	His438	H-acc	3.13
L_{10}	O1	OG1	Thr120	H-don	2.59
L_{11}	N1	OG	Ser198	H-don	2.60
	N5	OH	His438	H-don	2.66
L_{12}	-	-	-	-	-
L_{13},	-	-	-	-	-

Docking studies of ligands (**L_{1-13}**) with **1EVE** showed the presence of hydrogen bonding between these compounds with the protein of **1EVE**. It is revealed that the L_3 makes four hydrogen bonds interactions at the active-site gorge of the enzyme (**1EVE)**. We found four inter-hydrogen bonding formed between Tyr121(3.09Å) ,Ser200(2.85Å), His440(3.07Å) ,Gly118(2.75Å) amino acids and L_3. The same we noted that L_4 forms only one hydrogen bond with Tyr121(3.10Å). Also we noted that the native ligand (L_{13}: Donepezil) has one Tyr121(3.01Å).

Anne Imberty *et al* [66] showed that if the values of the distances from the hydrogen bonds belong to the interval: 2.5Å ≤ x ≤3.1Å : considered strong interactions. 3.1Å≤ x ≤3.55Å : supposed like averages interactions. >3.55Å : weak interactions. It is noticed that the values obtained of distances from the hydrogen bonds between the L_3 and the residues of active site belong to the interval 2.5Å ≤ x ≤ 3.1Å. These results indicate that the strong affinity of L_3 and L_4 on 1EVE could lead to the potent inhibition of the catalytic activity of the enzyme.

Table 9 and Figure 5 show the hydrogen bonds (*Atom of compound, involved receptor atoms, involved receptor residues, Type of Hydrogen bond and distances*) between the docked ligand and the amino acids of BuChE.

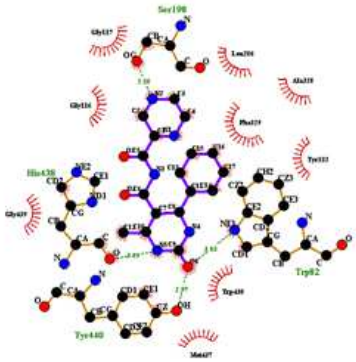

L1

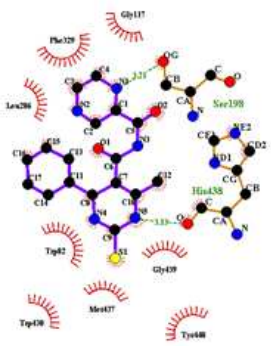

L2

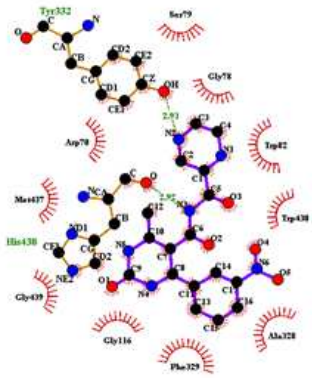

L3

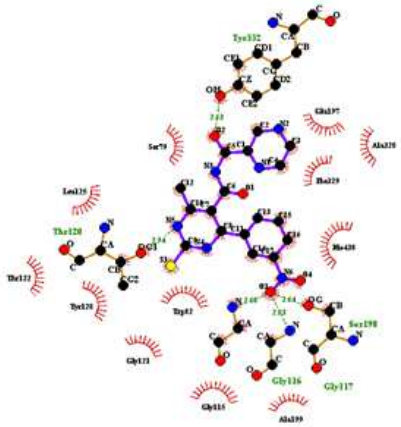

L4

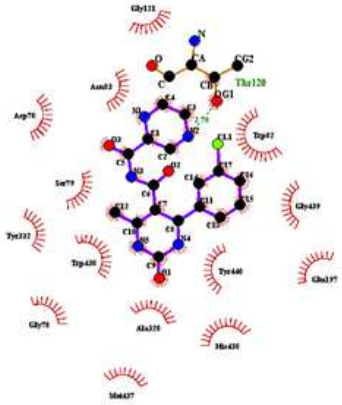

L5

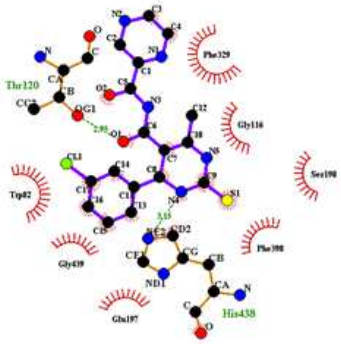

L6

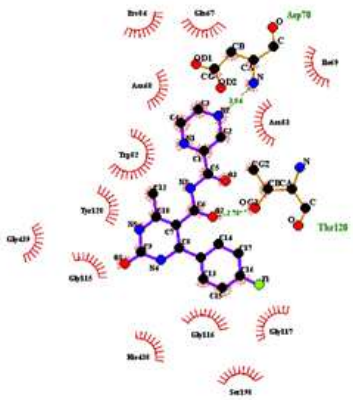

L7

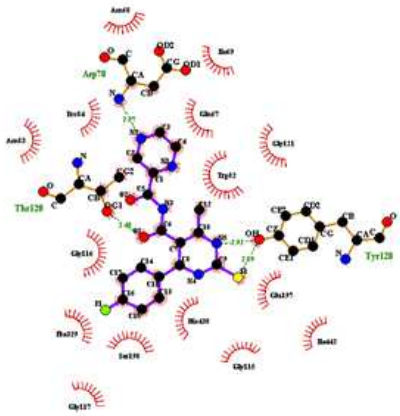

L8

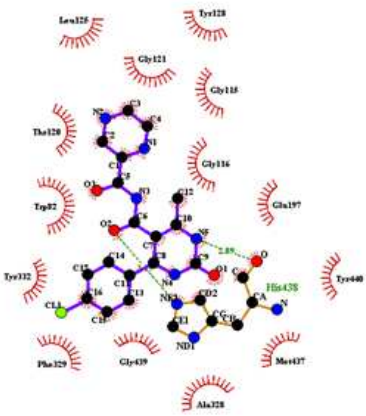

L9

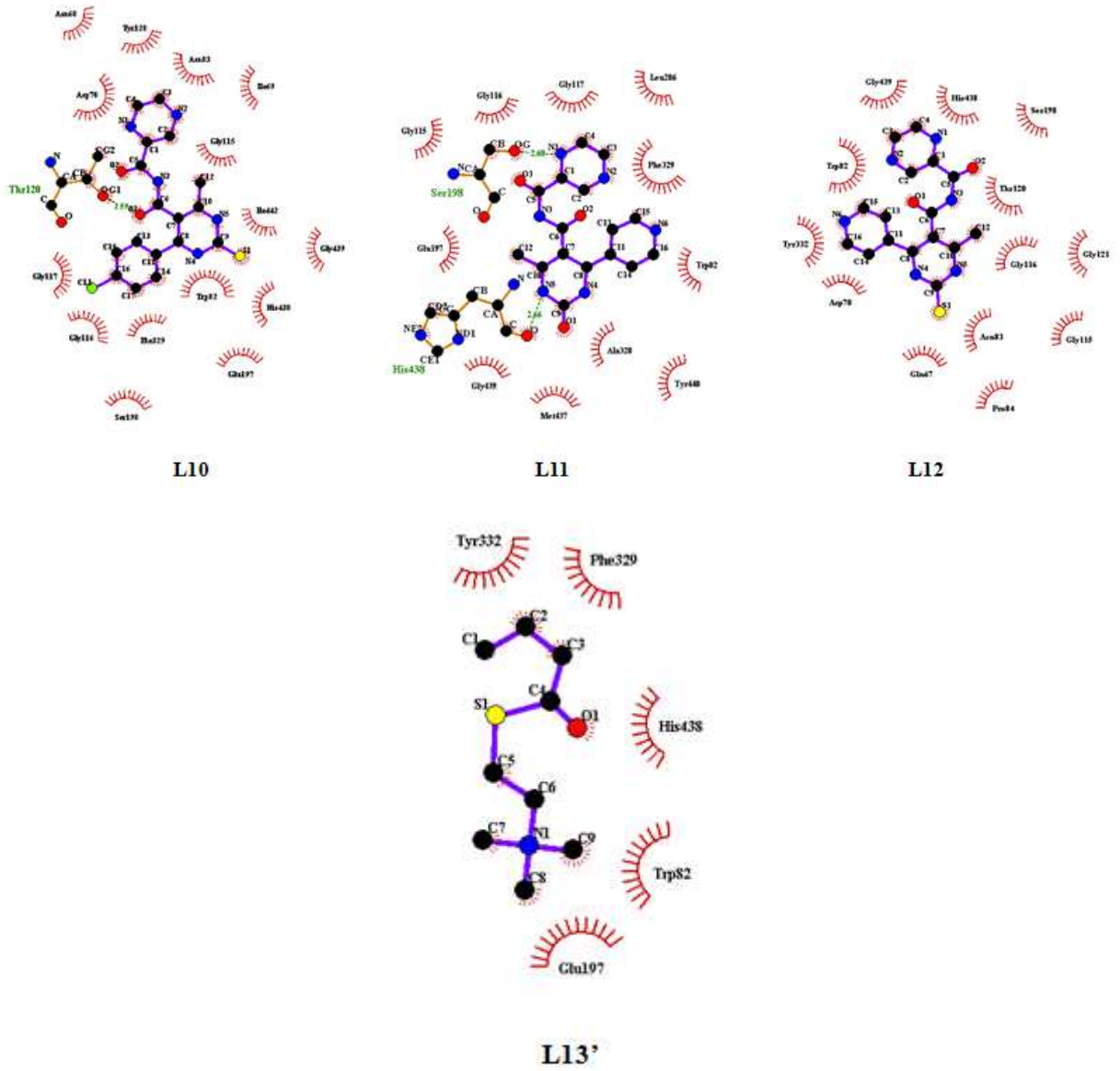

Figure 5 : Hydrogen bonds between ligands and residues of active site of 1P0P used LigPlot+ program [65].

The L_3 makes two hydrogen bonds interactions at the active-site gorge of the enzyme (**1P0P)**. We found four inter-hydrogen bonding formed between Tyr332(2.93Å) ,His438(2.92Å) amino acids and L_3. The same we noted that L_4 forms five hydrogen bonds with Tyr332(2.63Å), Ser198(2.64Å), Gly117(2.83Å), Gly116(2.60Å) and Tyr120(2.94Å). Also we noted that the native ligand ($L_{13'}$:BCH_604) $C_9H_{20}NOS$ has not hydrogen bonds. The same we noted that distances of hydrogen bonds belong to the interval $2.5Å \leq x \leq 3.1Å$, this confirm that L_3 and L_4 have a strongly interaction with active site of **1P0P.**

CONCLUSION

The docking studies as described above provide estimation on inhibitory activities of the docked ligand. The results showed that the series of novel pyrazinamide derivatives ($L_{1\text{-}12}$) fits well in the active site of both cholinesterase enzymes acetylcholinesterase (AChE) and butyrylcholinesterase (BuChE) and also interact with the residues in the active site which are important for their biological activity. Therefore these series of novel pyrazinamide compounds could be a putative inhibitor of both cholinesterase and might be used as anti-cholinesterase drug candidates.

In this paper, we report new template starting points for inhibitors of both receptors cholinesterase and a potential therapeutic target for the treatment of Alzheimer's disease.

It is noticed that the compounds L_3 and L_4 have the lowest values of energy MolDock score than the reference ligand

L_{13} (Donepezil) and $L_{13'}$ (BCH_604) and formed many interaction with residues of active site. These results indicate that L_3 and L_4 act as potential binding sites for the design of highly selective and potent both enzymes AChE and BuChE inhibitors in the active site.

Hence, it is concluded that L_3 and L_4 could be a potent ANTI-ALZHEIMER DRUG target molecule gainst AChE and BuChE which may be worth for further clinical trials.

REFERENCES

[1] C. Mount, C. Downton, *J. Nat. Med.*, **2006**, 12, 780-784.
[2] BC. Dickerson, A. Bakkour, DH. Salat, E. Feczko, J. Pacheco, DN. Greve, F. Grodstein, CI. Wright, D. Blacker, HD. Rosas, RA. Sperling, A. Atri, JH. Growdon , BT. Hyman, JC. Morris, B. Fischl, RL. Buckner, *Cereb. Cortex*., **2009**, 19, 497-510.
[3] SW. Scheff, DA. Price, *Neurobiol. Aging.*, **2003**, 24 ,1029-1046.
[4] J. Hardy, DJ. Selkoe. *Science.*, **2002**, 297 ,353-356.
[5] NH. Greig, K. Sambamurti, QS. Yu, A. Brossi, GB. Bruinsma, DK. Lahiri. *Curr. Alzheimer.Res*.,**2005**, 2 ,281–290.
[6] DK. Lahiri, MR. Farlow, N. Hintz, T. Utsuki, NH. Greig. *Acta Neurol. Scand. Suppl* .,**2000**, 176 ,60–67.
[7] JA. Guevara-Salazar, M. Espinoza-Fonseca, HI. Beltran, J. Correa-Basurto, JG. Trujillo-Ferrara. *J. Mex. Chem. Soc.*, **2007**, 51 ,173–177.
[8] E. Giacobini. *Pharm. Res.*, **2004**, 50 ,433-440.
[9] E. Giacobini, R. Spiegel, A. Enz, AE. Veroff, NRJ. Cutler. *Neural Trans.*, **2002**, 109 ,1053-1065.
[10] MM. Mesulam, A. Guillozet, P. Shaw, A. Levey, EG. Duysen, O. Lockridge. *Neuroscience*., **2002**, 110 ,627-639.
[11] H. Sugimoto, Y. Yamanishi, Y. Iimura, Y. Kawakami. *Curr. Med. Chem.*, **2000**, **7** ,303-339.
[12] P. Camps, X. Formosa, C. Galdeano, T. Gomez, D. Munoz-Torrero, L. Ramirez, E. Viayna, E. Gomez, N. Isambert, R. Lavilla, A. Badia, M. Victoria Clos, M. Bartolini, F. Mancini, V. Andrisano, A. Bidon-Chanal, O. Huertas, T. Dafni, F. Javier Luque. *Chem. Biol. Interact.*, **2010**, 187 ,411-415.
[13] S. Kavanagh, M. Gaudig, B. Van Baelen, M. Adami, A. Delgado, C. Guzman, E. Jedenius, B. Schaeuble. *Acta Neurol. Scand*., **2011**, 124 ,302-308.
[14] R. Hoerr, M. Noeldner, Ensaculin (KA-672 center dot HCl). *CNS Drug Rev*., **2002**, 8 ,143-158.
[15] NH. Greig, T. Utsuki, QS. Yu, X. Zhu, HW. Holloway, T. Perry, B. Lee, DK. Ingram, DK. Lahiri.*Curr. Med. Res. Opin*., **2001**, 17 ,159-165.
[16] S. Hosseini, M. Monajjemi, E. Rajaeian, M. Haghgu, AA. Salari, MR. Gholami. *Ira. J. Pharm. Res*., **2013**, 12 ,745–750.
[17] B. Desai, D. Sureja, Y. Naliapara, A. Shah, AK. Saxena. *Bio. Med. Chem* ., **2001**, 9 ,1993–1998.
[18] K. Singh, B. Wan, S. Franzblau, K. Chibale. *Bio. Med. Chem. Lett.*, **2011**, 46 ,2290–2294.
[19] AD. Baldev, KB. Vyas, KB. Patel, KS. Nimavat. *J. Chem. Pharm. Res*., **2012**, 4, 2972–2978.
[20] MK. Hossain, H. Bhuiyan, KM. Mizanur Rahman., MK. Hossain, A. Rahim. *Acta Pharm.*, **2006**, 56 ,441–450.
[21] NS. Shetty, RS. Lamani, IAM. Khazi. *J. Chem. Sci.*, **2009**, 121,301–307.
[22] P. Sharma, N. Rane, VK. Gurram. *Bio. Med. Chem. Lett.*, **2004**, 14, 4185–4190.
[23] WA. El-Sayed, OM. Ali, RAF. Zyada, AA. Mohamed, AAH. Abdel-Rahman. *Acta Pol. Pharm*., **2012**, 69, 439–447.
[24] RJ. Gillespie, IA. Cliffe, CE. Dawson. *Bio. Med. Chem. Lett*., **2008**, 18, 2924–2929.
[25] A. Orjales, R. Mosquera, B. Lopez, R. Olivera. *Bio. Med. Chem*., **2008**, 16, 2183–2199.
[26] EP. da, S. Falcao, SJ. de Melo, RM. Srivastava. *Eur. J. Med. Chem*., **2006**, 41, 276–282.
[27] A. Gangjee, Y. Zhao, S. Raghavan, MA. Ihnat, BC. Disch. *Bio. Med. Chem*., **2010**, 18, 5261–5273.
[28] H. Parveen, F. Hayat, A. Salahuddin, A. Azam. *Eur. J. Med. Chem*., **2010**, 45, 3497–3503.
[29] F. Xie, H. Zhao, L. Zhao, L. Lou, Y. Hu. *Bio. Med. Chem. Lett*., **2009**, 19, 275–278.
[30] TS. Jyostna, G. Achaiah. *Eur J. Med. Chem*., **2010**, 45, 1453–1458.
[31] A. Basiri, V. Murugaiyah, H. Osman, RS. Kumar, Y. Kia, KB. Awang, MA. Ali. *Eur. J. Med. Chem*., **2013**, 67, 221–229.
[32] E. Karthikeyan, AA. Mohammed, E. Manogaran, E. Kalpana, S. Sivaneswari. *Biotechnology Reports*., **2015**, 5, 1–6.
[33] Hyperchem 7.0, Hypercube Inc.
[34] G. Kryge, I. Silman, JL. Sussman**.** *Structure. Fold. Des*., **1999**, *7*, 297-307.
[35] Y. Nicolet, O. Lockridge, P. Masson, JC. Fontecilla-Camps, F. Nachon. *J. Biol. Chem*., **2003**, 278, 41141-41147.
[36] 1EVE and 1P0P: 3-dimensional structure downloaded from http://www.rcsb.org/pdb.
[37] SJ. Weiner, PA. Kollman, T. Nguyent, DA. Case. *J. Comput .Chem*., **1986**, 7, 230-252.

[38] EF. Pettersen, TD. Goddard, CC. Huang, GS. Couch, DM. Greenblatt, EC. Meng, et al. *J. Comput. Chem.*, **2004**, 25, 1605–1612.
[39] FFda. Elaine, FB. Edilaine, AO. Aline, CR. Teodorico. *J. Biom. Struct. Dyn..*, **2010**, 27, 619–625.
[40] R. Thomsen, MH. Christensen. *J. Med. Chem*., **2006**, 49, 3315-3321
[41] H. Schulz, E. Dale, Y. Karimi-Nejad, C. Oefner. *J. Mol. Biol*., **2009**, 385, 178–187.
[42] JK. Labanowski, JW. Andzelm. Density Functional Methods in Chemistry., **1991**, New York: Springer Verlag.
[43] MJ. Frisch, GW. Trucks, HB. Schlegel, GE. Scuseria, MA. Robb, JR. Cheeseman et al., Gaussian 09, Revision A.02, Gaussian Inc, Wallingford CT, **2009**.
[44] LA. Curtiss, C. Jones, GW. Trucks, K. Raghavachari, JA. Pople. *J. Chem. Phys.*, **1990**, 93, 2537–2545.
[45] R. Ditchfield, WJ. Hehre, JA. Pople. *J. Chem. Phy.*, **1971**, 54, 724–728.
[46] WJ. Hehre, R. Ditchfield, JA. Pople. *J. Chem. Phys.*, **1972**, 56, 2257–2261.
[47] PC. Hariharan, JA. Pople. *Mol. Phys*., **1974**, 27, 209–214.
[48] MS. Gordon. *Chem. Phys. Lett*., **1980**, 76, 163–168.
[49] PC. Hariharan, JA. Pople. *Theo. Chim. Acta*., **1973**, 28, 213–222.
[50] RC. Binning Jr, LA. Curtiss. *J. Comp. Chem*., **1990**, 11, 1206–1216.
[51] AD. McLean, GS. Chandle. *J. Chem. Phys*., **1980**, 72, 5639– 5648.
[52] W. Kohn, AD. Becke, RG. Parr. *J. Phys. Chem.*, **1996**, 100, 12974–12980.
[53] RG. Parr, LV. Szentpály, S. Liu. *J. Am. Chem. Soc*., **1999**, 121, 1922–1924.
[54] RG. Parr, RA. Donnelly, M. Levy, WE. Palke. *J. Chem. Phys*., **1978**, 68, 3801–3807.
[55] I. Fleming. Frontier Orbitals and Organic Chemical Reactions. John & Sons; New York ., **1976**. Wiley
[56] I. Daoud, M. Mesmoudi, S. Ghalem. *International Journal of Chemical and Analytical Science*., **2013**, 4, 49-56.
[57] S. Liao, H. Deng, S. Huang, J. Yang, S. Wang, B. Yin, T. Zheng, D. Zhang, J. Liu, G. Gao, J. Ma, Z. Deng. *Bioorganic & Medicinal Chemistry Letters*., **2015**, 25, 1541–1545.
[58] AW. Ckowska, WK. Ckowski, M. Bajda, B. Brus, P. Czerwin´ska, S. Gobec, B. Filipek, K. Salat, B. Malawska. *Bioorganic & Medicinal Chemistry*., **2015**, 23, 2445–2457.
[59] N. Guzior, M. Bajda, J. Rakoczy, B. Brus, S. Gobec, B. Malawska. *Bioorganic & Medicinal Chemistry*., **2015**, 23, 1629–1637.
[60] MT. Hassan Khan. *New Biotechnology*., **2009**, 25, 5.
[61] T. Murakawa, Y. Matsushita, T. Suzuki, MT. Hassan Khan, N. Kurita. *Journal of Molecular Graphics and Modelling*., **2014**, 54, 54–61
[62] A. Basiri, V. Murugaiyah, H. Osman, RS. Kumar, Y. Kia, A. Hooda, RB. Parsons. *Bioorganic & Medicinal Chemistry*., **2014**, 22, 906–916.
[63] F. Zheng, M. Zhan, X. Huang, M. Diwan, M. Abdul Hameed, CG. Zhan. *Bioorganic & Medicinal Chemistry*., **2014**, 22, 538–549.
[64] I. Abdelli, Mohammad A. Kamal, I. Daoud, S. Ghalem, M. Merad. *Der Pharma Chemica.*, **2015**, 7(8),181-186.
[65] RA. Laskowski, MB. Swindells. *J. Chem. Inf. Model*., **2011**, 51, 2778–2786.
[66] A. Imberty, KD. Hardman, JP. Carver, S. Pérez. *Glycobiology*., **1991**, 1, 631-642.